

Title: Parametric Instability in Future Gravitational Wave Detectors

Date: Jun 12, 2018 02:00 PM

URL: <http://pirsa.org/18060053>

Abstract:

Contents

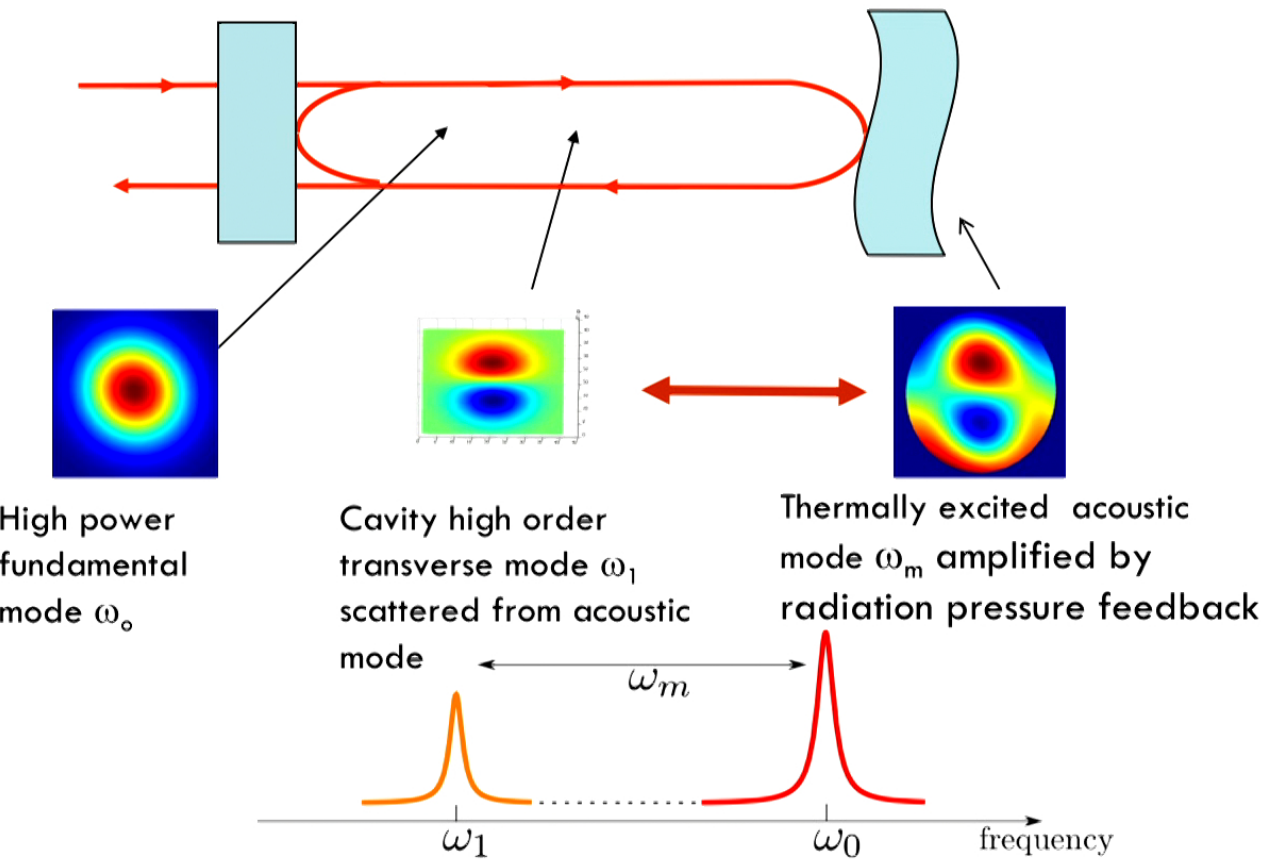
2

- Parametric instability (PI) and observation results
- Current PI control at aLIGO
 - Thermal tuning, Electrostatic feedback, Acoustic mode damper (AMD)
- AMD potential thermal noise implications
- PI simulation results of Voyager
- PI simulation results of CE
- Mechanical resonators for optomechanical filter

Path to kHz GW detectors

Parametric Instability

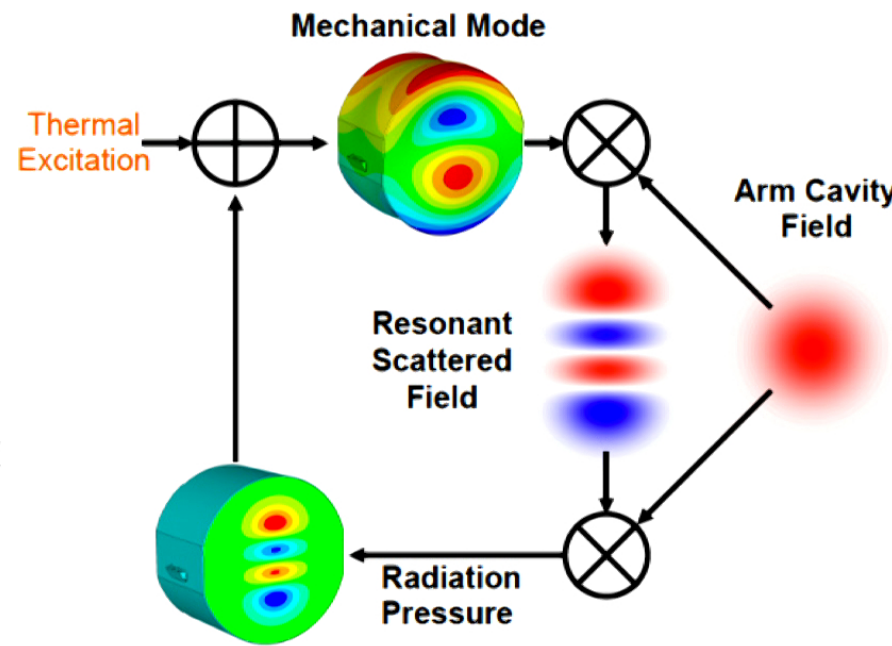
3



Parametric Instability

4

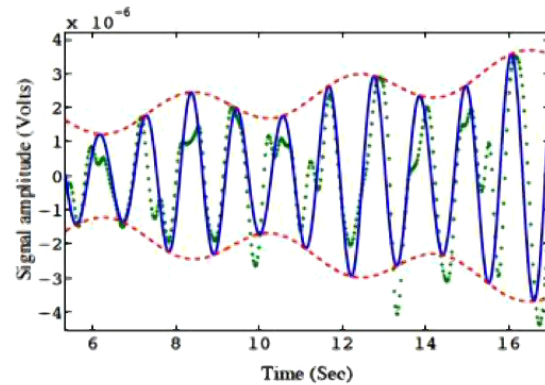
The parametric instability can be described as a classical feedback phenomenon.



M. Evans, L. Barsotti, P. Fritschel, Physics Letters A 374 (2010) 665–671
Path to kHz GW detectors

Parametric Instability at Gingin 80m

5

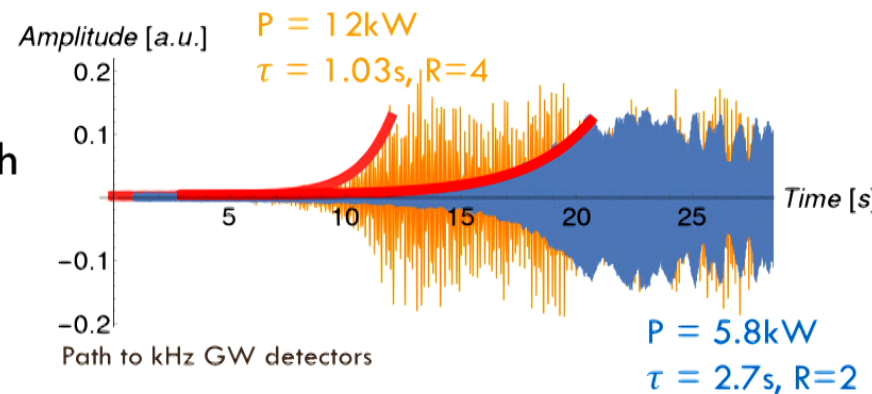


Observation of parametric instability and modulation effect

C. Zhao et al. *Phys. Rev. D*, 2015

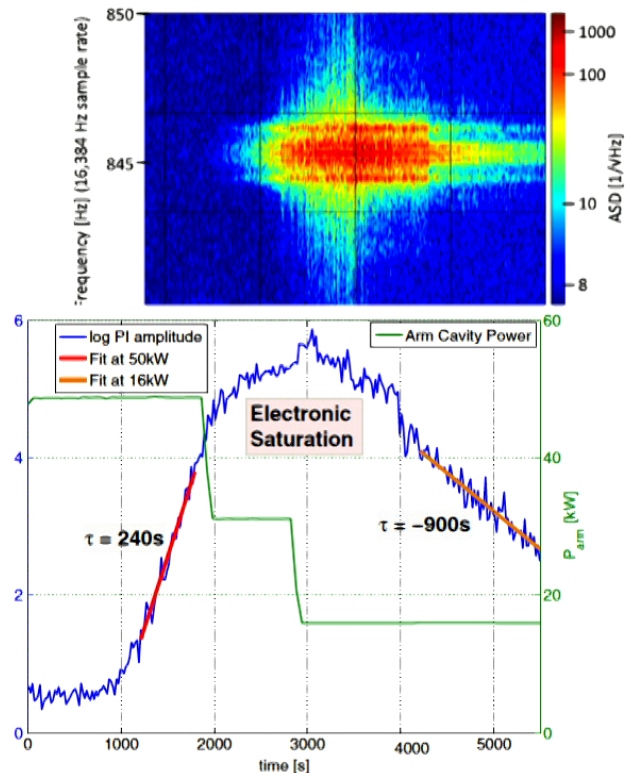
$R = 1.45$

Observation of strong parametric instability at high circulating power

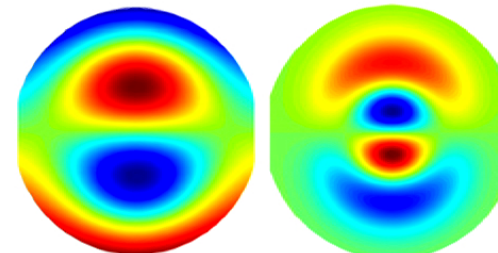


Parametric Instability at aLIGO

6



M. Evans, et al. Phys. Rev. Lett. 114, 161102



Mirror surface
displacement The 3rd order
optical mode

- PI exists
- Current power level
PI is controlled

Path to kHz GW detectors

Factors Affecting Parametric Gain

- Parametric gain

$$R = \pm \frac{8P_{in}Q_0Q_lQ_m}{L^2\omega_0\omega_m} \frac{\gamma B}{1+(\Delta\omega/\delta_l)^2}$$

$$\Delta\omega = \omega_m - (\omega_0 - \omega_{mn})$$

$$\omega_0 - \omega_a = \frac{c}{L}(m+n) \arccos \left(\pm \sqrt{\left(1 - \frac{L}{R_1}\right) \left(1 - \frac{L}{R_2}\right)} \right)$$

- Acoustic mode amplitude

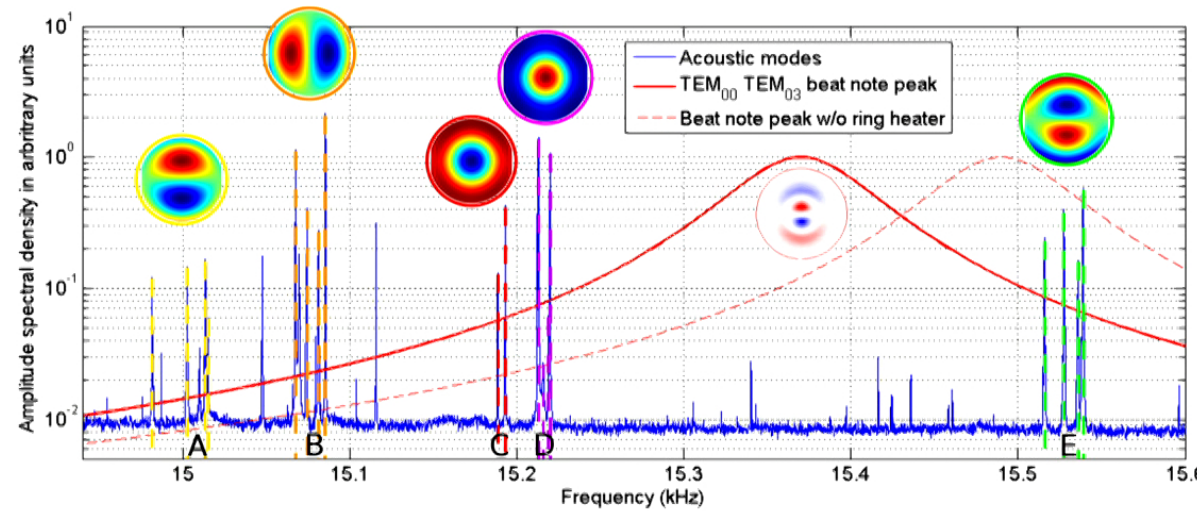
$$x \sim A e^{-(1-R)t/\tau}$$

Path to kHz GW detectors

- Control Strategies
 - Thermal tuning
 - Electrostatic feedback
 - Acoustic Mode Damper

Thermal tuning

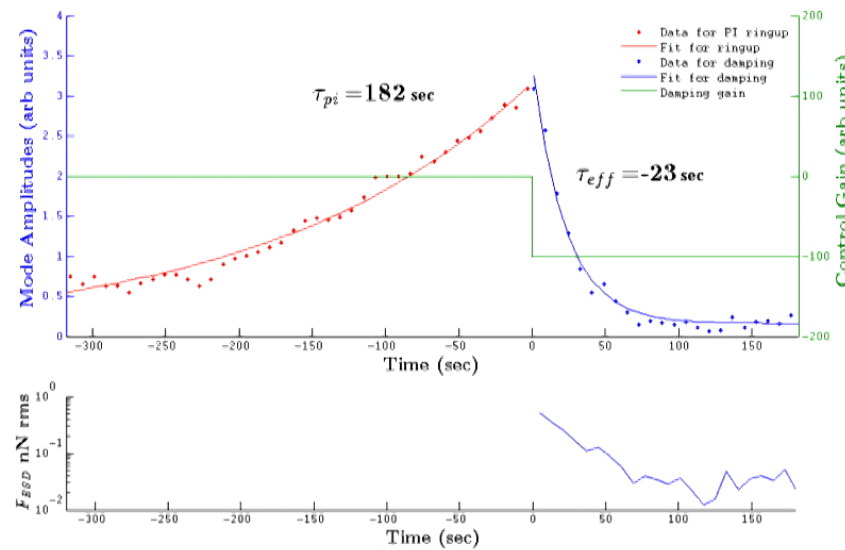
LLO: ring heaters tuned to no PI sweet spot



C. Blair: PRL 118, 151102 (2017)

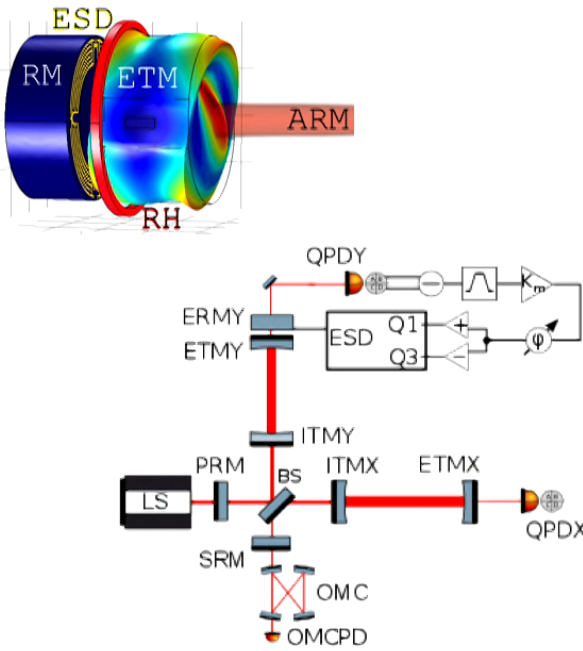
Electrostatic feedback

LHO: Electrostatic Drives used to
damp at 50W



C. Blair et al: PRL 118, 151102 (2017)

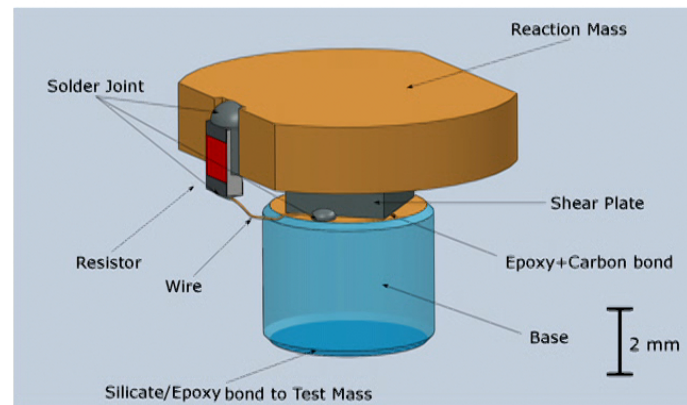
Path to kHz GW detectors



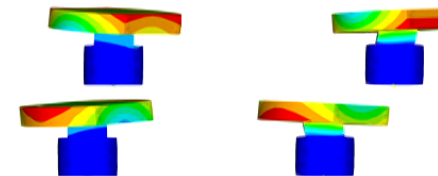
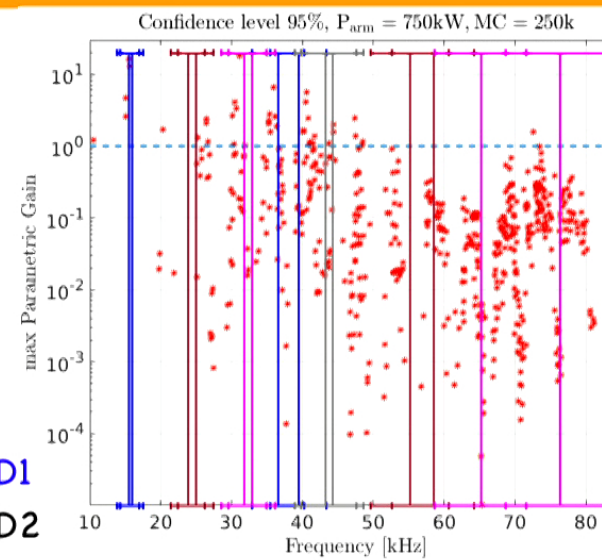
Acoustic Mode Dampers

10

- 4 AMD per test mass
- 4 damping modes per AMD
- 1.5% predicted thermal noise impact



■ AMD1
■ AMD2
■ AMD3
■ AMD4



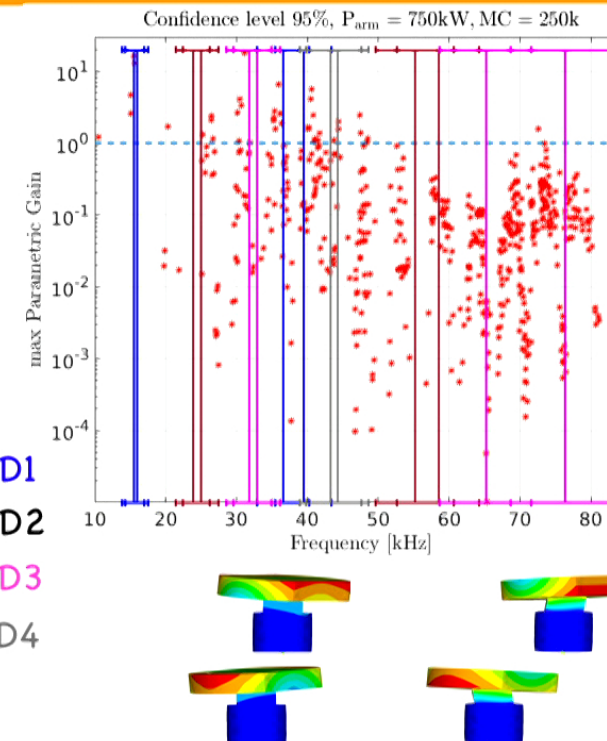
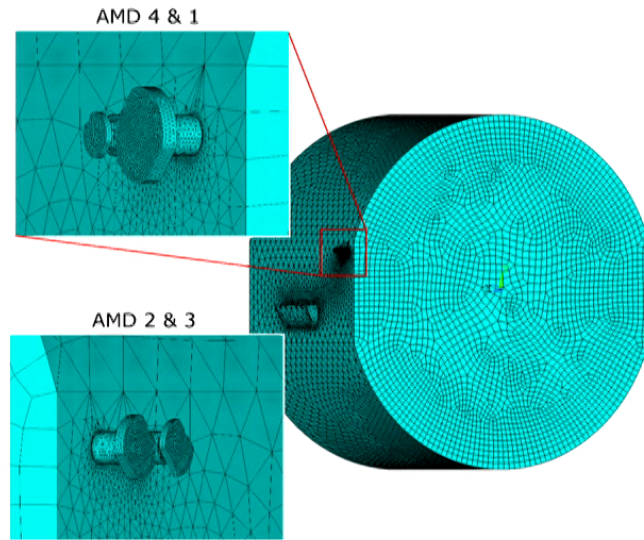
LIGO Document G1800454-v1 and, G1800975

Path to kHz GW detectors

Acoustic Mode Dampers

10

- 4 AMD per test mass
- 4 damping modes per AMD
- 1.5% predicted thermal noise impact



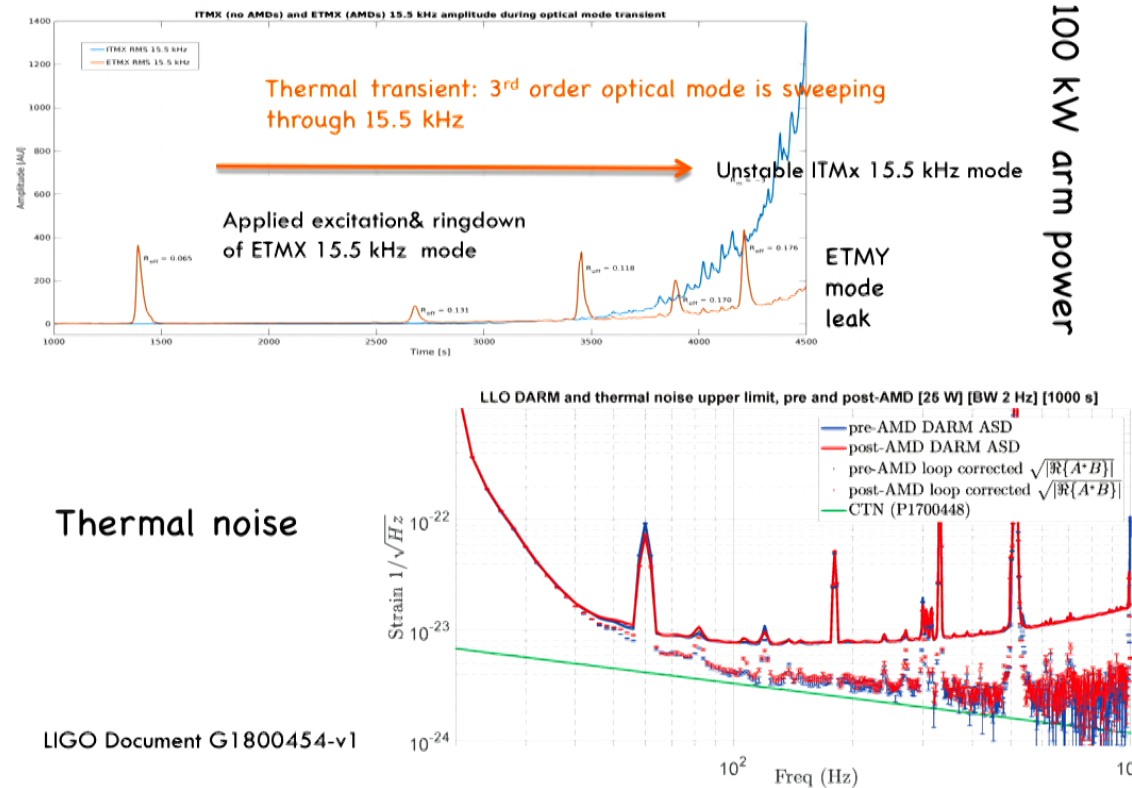
LIGO Document G1800454-v1 and, G1800975

Path to kHz GW detectors

Acoustic Mode Dampers

11

Stability of 15.5 kHz mode: ITMX vs ETMX

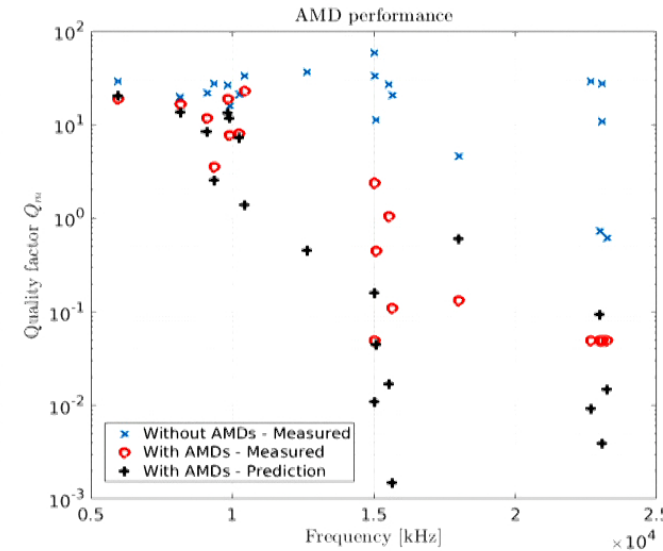


Acoustic Mode Dampers

12

Before AMDs (measured) & After (measured & predicted)

freq (Hz)	mode #	Pre-AMD Q ($\times 10^6$)	Post-AMD Q ($\times 10^6$)	Predicted Post-AMD Q ($\times 10^6$)
5948	1	29.3	19.1	20.3
6050			18.7	
8158	3	20.2	16.7	13.8
9101	6	21.8	11.8	8.5
9338	7	27.6	3.55	2.6
9827	9	26.9	18.9	13.5
9878	10	15.7	7.73	11.8
10216	11	21.2	8.03	7.3
10424	12	33.3	22.8	1.4
12627	15	36.7		0.46
15006	30	59.3	2.39	0.011
15017	31	33.2	NA (ETMY)	0.16
15071	32	11.4	0.45	0.045
15538	36	27.1	1.05	0.017
15630	37	20.6	0.11	0.0015
18001	50	4.65	0.134	0.61
18051		<0.04		
22662	84	29.1	NA(<0.1)	0.0093
22969	87	0.73	NA(<0.1)	0.095
23049	88	10.9	NA(<0.1)	0.004
23060		28	NA (ETMY)	0.004
23222	89	0.62	NA(<0.1)	0.015
38106		9.5	0.019	
47468		2.3	0.03	
47485		5.3	0.041	



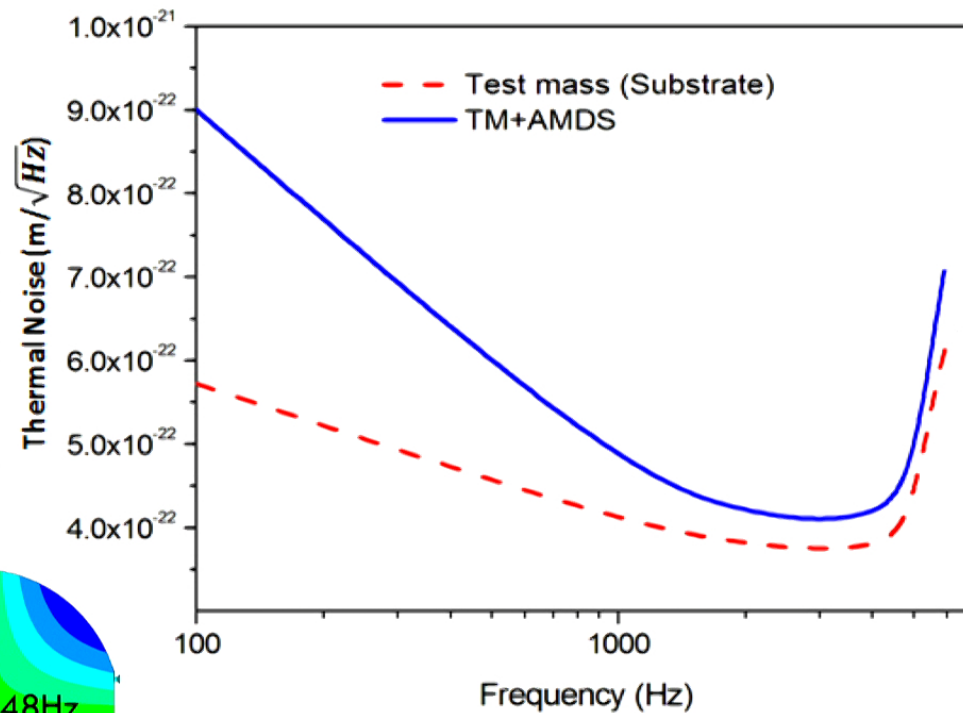
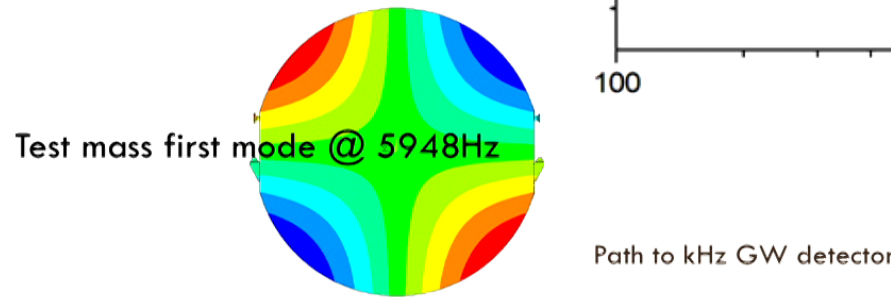
LIGO Document G1800454-v1

Path to kHz GW detectors

Preliminary FEM simulation of AMD thermal noise contribution

13

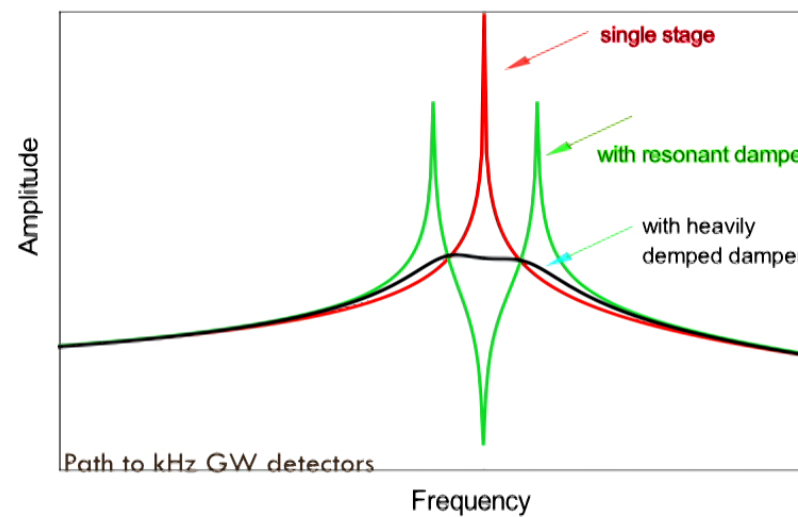
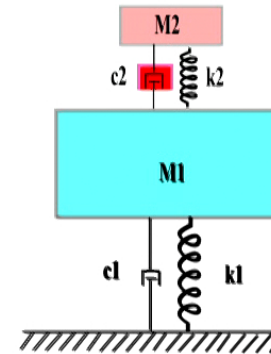
- FEM simulation shows the first TM internal mode dominates the thermal noise contribution at around 5.9 kHz (no coating thermal noise included)



Resonant Damper-one dimensional model

14

- One dimensional model—single stage
 - M1: test mass
 - M2: Damper
 - Heavily damped damper
 - Lossy damper in direct contact with the test mass
 - Thermal noise?

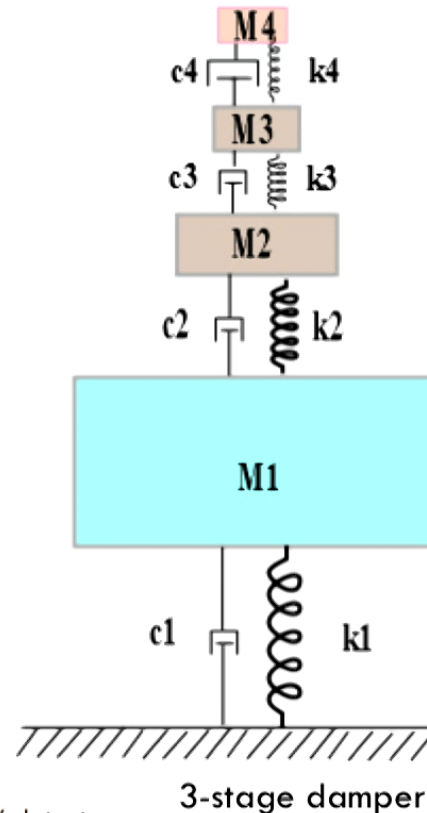


Li Ju G1700852

Is it possible to improve?

15

- Multi-Stage Damper
- Only the last stage is lossy
- Very small lossy stage to achieve effective damping



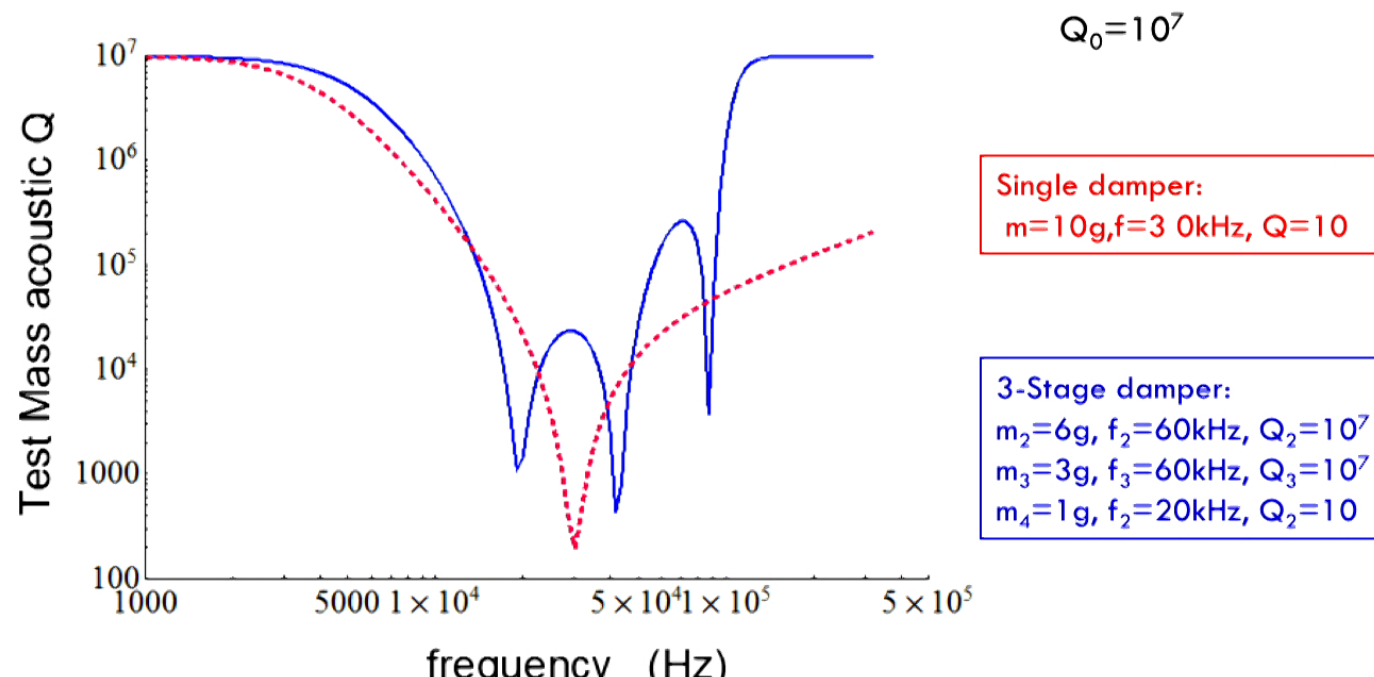
Li Ju G1700852

Path to kHz GW detectors

One dimensional acoustic modes

Q estimation

16



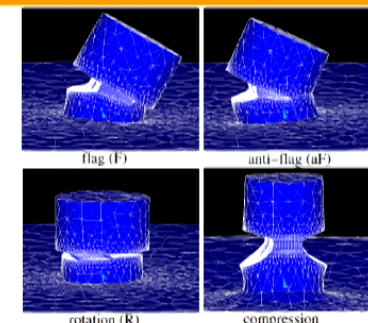
Li Ju G1700852

Path to kHz GW detectors

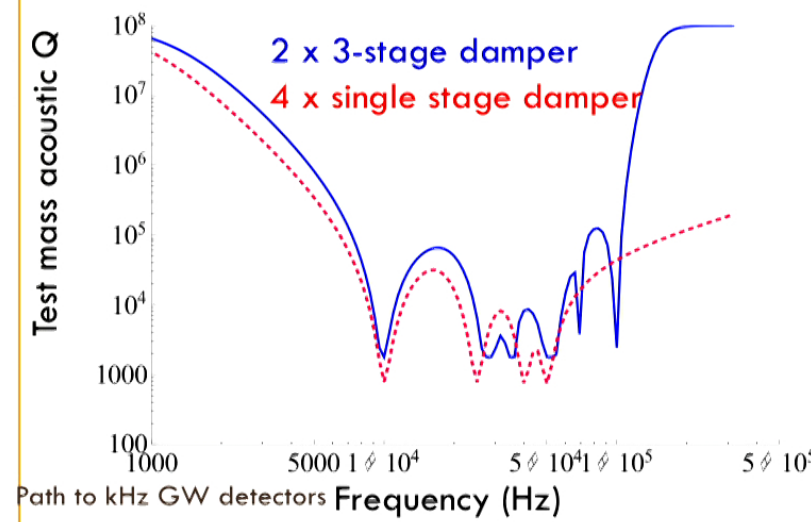
Multiple multi-stage

17

- 3D single stage = effective a couple of dampers
- For high Q damper, could use multiple multi-stage dampers



S. Gras, et. al. PRD, **92**, 082001 (2015)

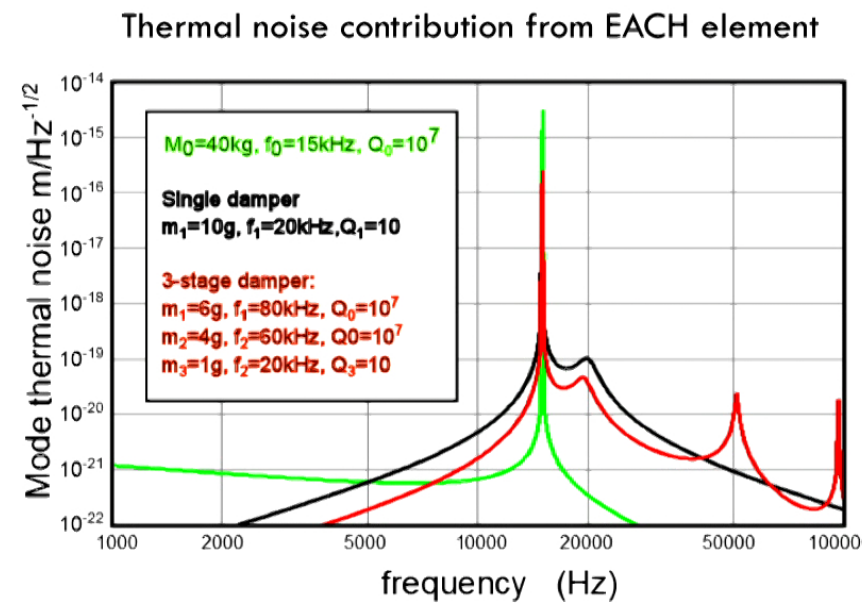


Li Ju G1700852

Thermal noise rough estimation

18

- Example for a single acoustic mode
- Multi-stage damper has lower thermal noise contribution
- Over simplified model here
- Need more detailed thermal noise analysis for multi-stage damper

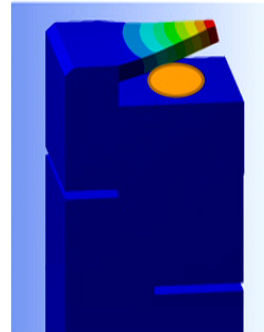


Li Ju G1700852

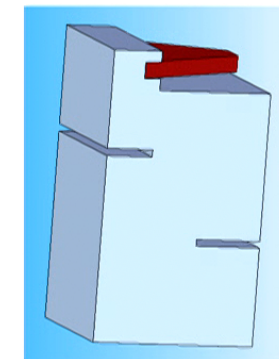
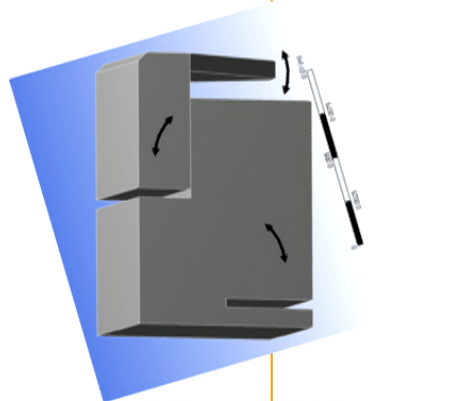
Practical design

19

- Monolithic high Q metal
- Electrical discharge
Machining
- Using magnet eddy-current
damping
- Monolithic high Q material
- Last stage with different lossy
material (Viton) tight fit



Li Ju G1700852



PI simulation for Voyager: simple cavity

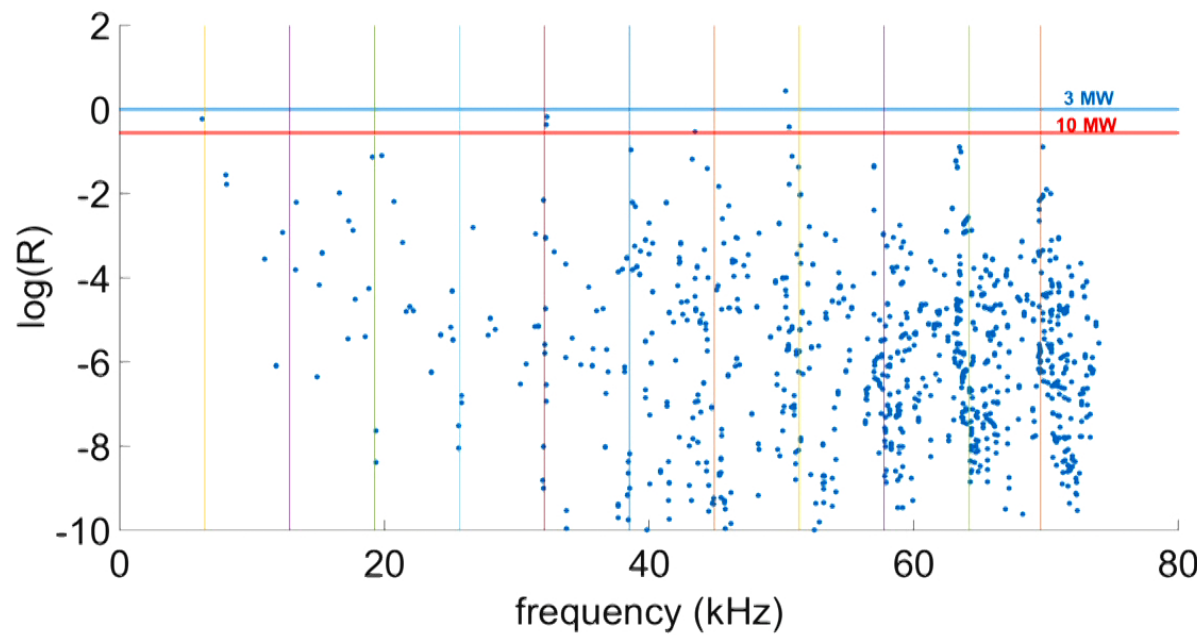
Parameters:

- laser wavelength : $2 \mu\text{m}$
- Large Silicon mirror: 204 kg
- Cryogenic : at 123 K
- Assume $Q \sim 10^7$ after all coatings
- High power laser: Arm cavity powers will reach $\sim 3/10 \text{ MW}$
- Mirror radius: 0.225m
- Mirror thickness: 0.55m
- Beam radius on ITM/ETM: $0.059\text{m}/0.084\text{m}$

Path to kHz GW detectors

PI simulation for Voyager: simple cavity

21

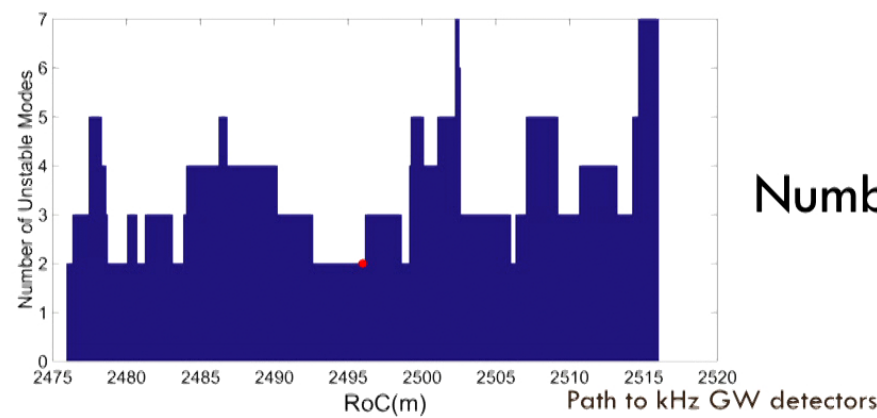
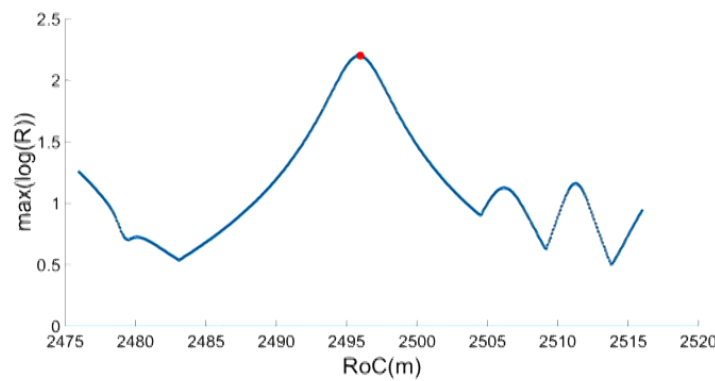


Path to kHz GW detectors

PI simulation for Voyager: simple cavity (3 MW circulating power)

22

Max R

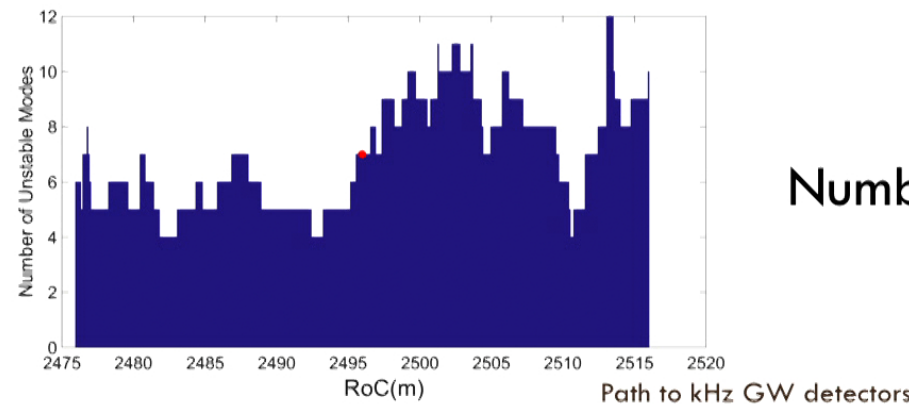
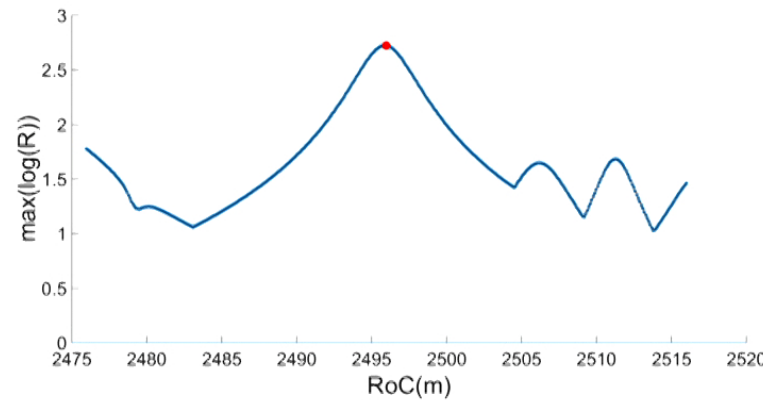


Number of unstable modes

PI simulation for Voyager: simple cavity (10 MW circulating power)

23

Max R

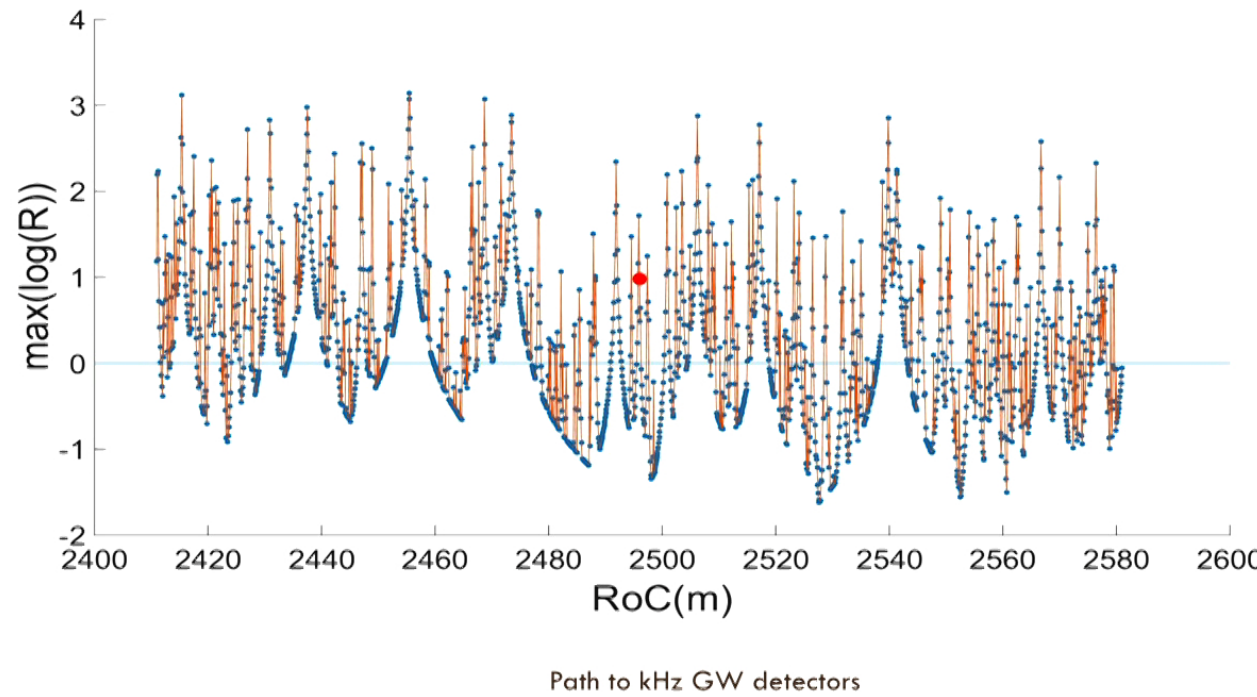


Number of unstable modes

PI simulation for Voyager: Dual-recycling

24

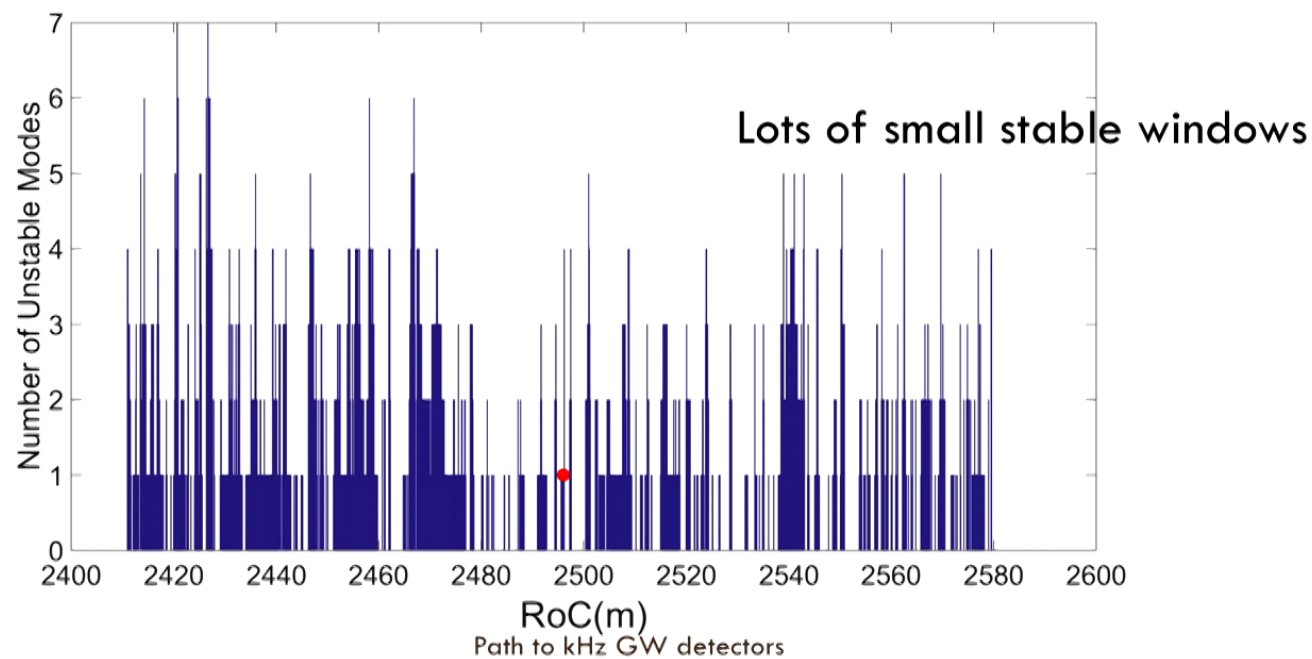
Assuming all high order modes are **resonant** in both PRC and SRC



PI simulation for Voyager: Dual-recycling

25

Assuming all high order modes are **resonant** in both PRC and SRC



PI simulation for 40km interferometer

26

Test mass parameters

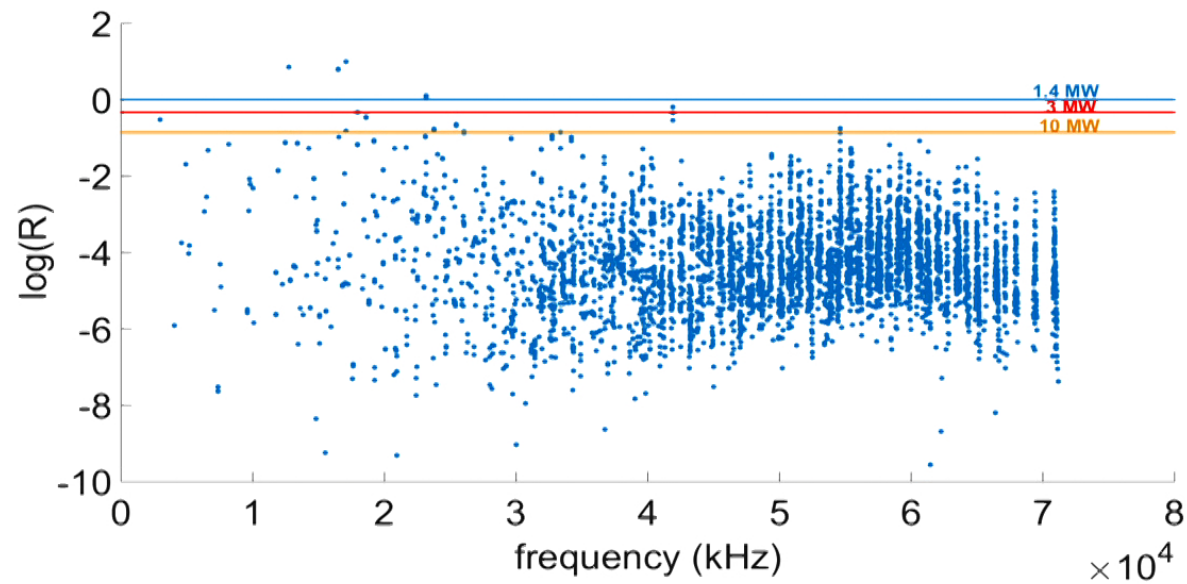
Radius of test mass	0.34 m
Thickness of test mass	0.4 m
Mass of test mass	322 kg
Cavity Length	40 km
Beam sizes on ITM/ETM	12 /12 cm

Path to kHz GW detectors

PI simulation for 40km: simple cavity

27

Parametric Gain



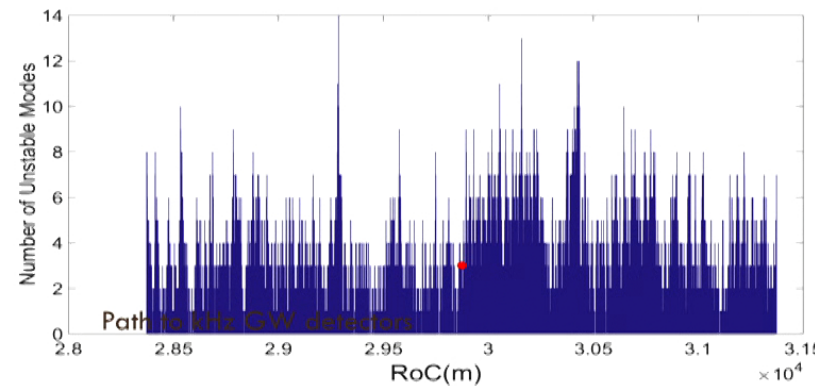
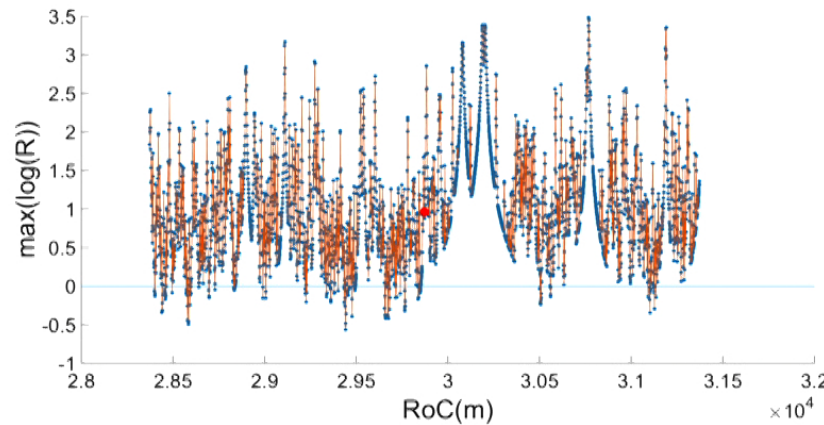
Path to kHz GW detectors

PI simulation for 40km: Dual-recycling

29

Assuming all high order modes are **resonant** in both PRC and SRC, @circulating power 3 MW

Windows of PI-free exit.



PI: Summary

30

- AMDs are promising to damp almost all unstable acoustic mode for current aLIGO;
- To damp low frequency unstable mode, the AMD may have potential to introduce extra thermal noise in the kHz band;
- Detailed FEM simulation is required to optimize the AMD design and to confirm the thermal noise contribution;
- For future detector design, may consider to choose PI free configuration through simulation, with optimized AMDs included.

Path to kHz GW detectors

Mechanical resonators for optomechanical filters

31

Requirements: Low mechanical and optical losses

SiN membrane:

PRL 116,147202 (2016)

140 kHz mode $Q \sim 100$ million,
optical reflectivity $> 99\%$ with photonic crystal

GaAs/AlGaAs:

a few hundred Hz mode, $Q \sim 10^4$; optical loss $\sim \text{ppm}$

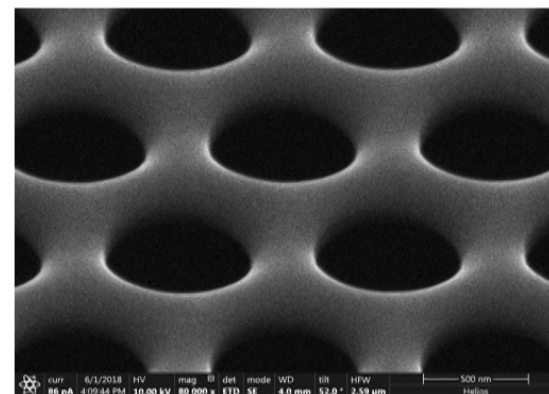
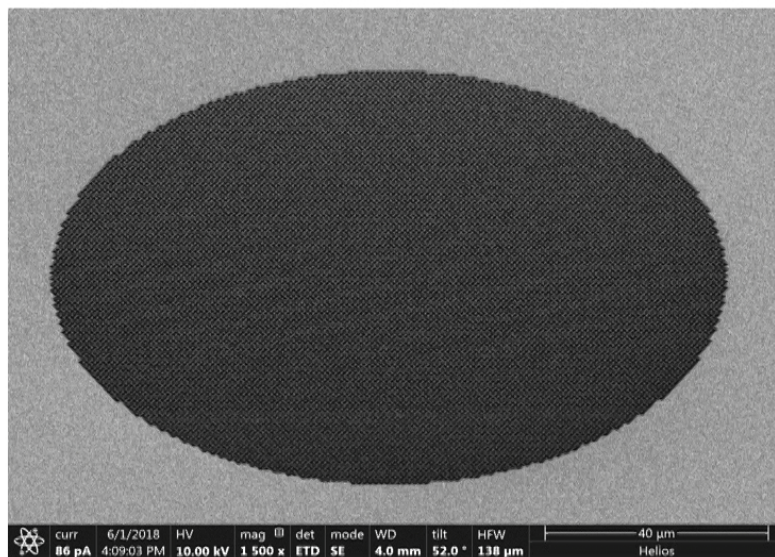
Next talk by Thomas

Path to kHz GW detectors

Mechanical resonators: SiN

32

0.1 mm diameter pattern on 200nm think SiN membrane
Machined by Focused Ion Beam (FIB)



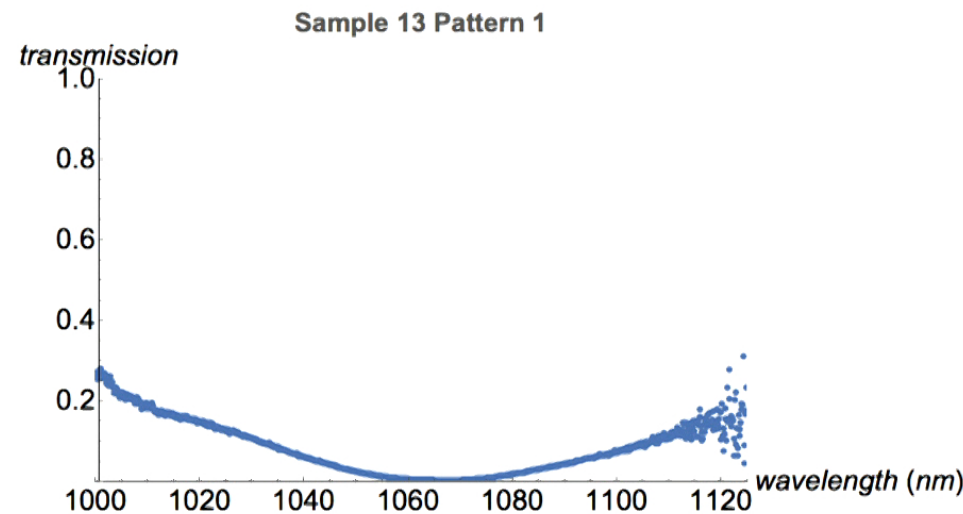
Zoom in of the structure:
~700nm diameter holes;
~1000nm gap.

Path to kHz GW detectors

Mechanical resonators: SiN

33

Optical reflectivity

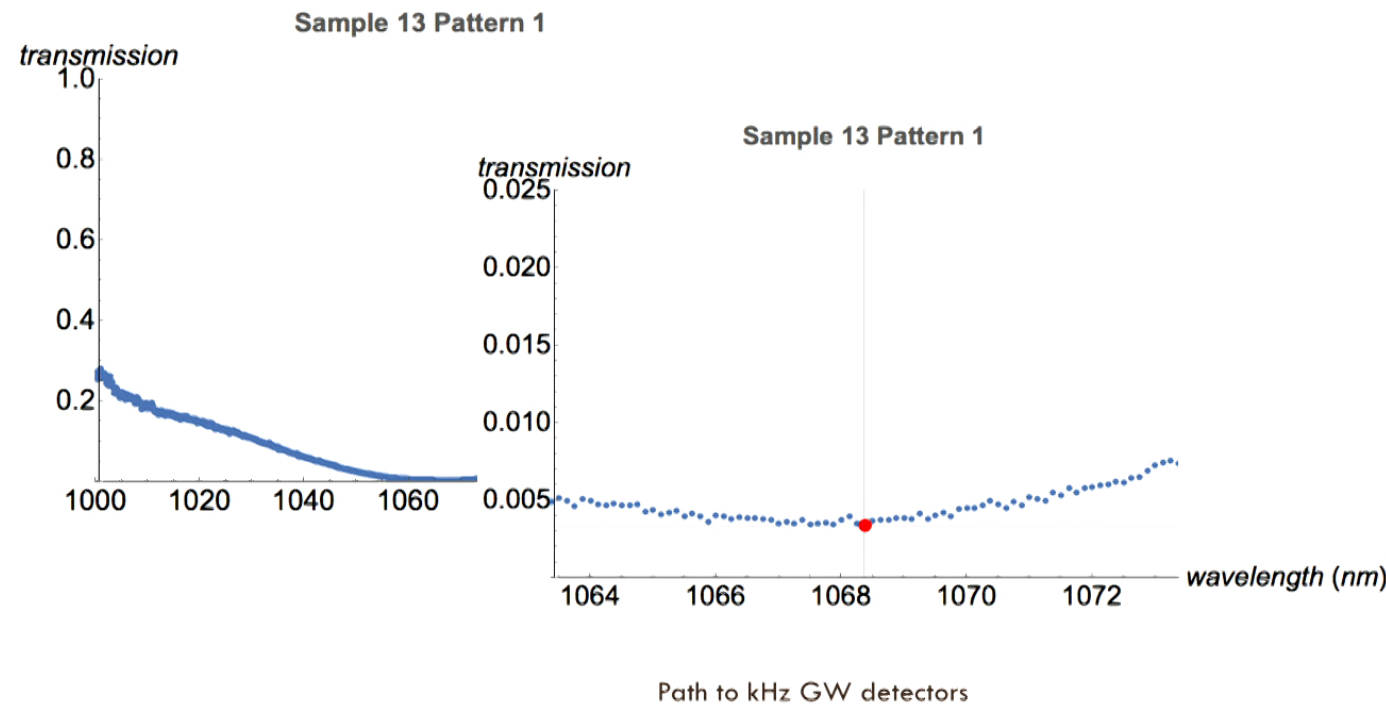


Path to kHz GW detectors

Mechanical resonators: SiN

33

Optical reflectivity



Mechanical resonators: AlGaAs/GaAs

34



Small mirror suspended by ribbons;
Optical dilution to high effective Q-factors

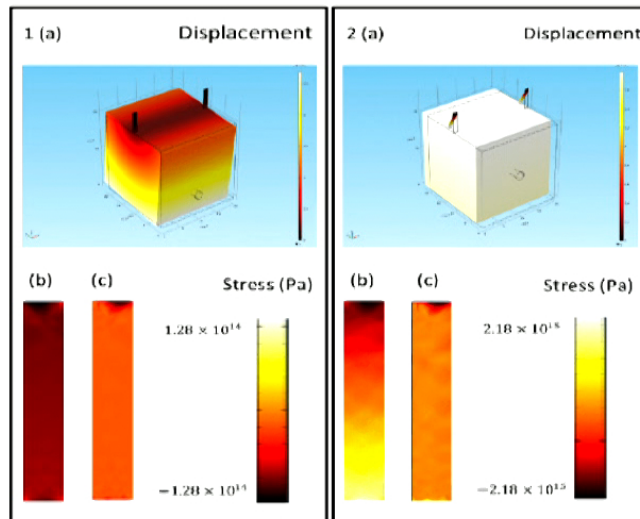
$$Q_{tot} = \frac{E_{int} + E_{sus} + E_{opt}}{\Delta E_{int} + \Delta E_{sus}}$$

Path to kHz GW detectors

Mechanical resonators

35

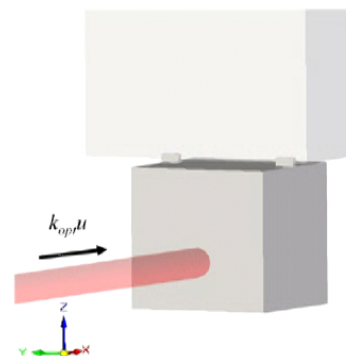
1) Central percussion issue:



Below central percussion

At the central percussion

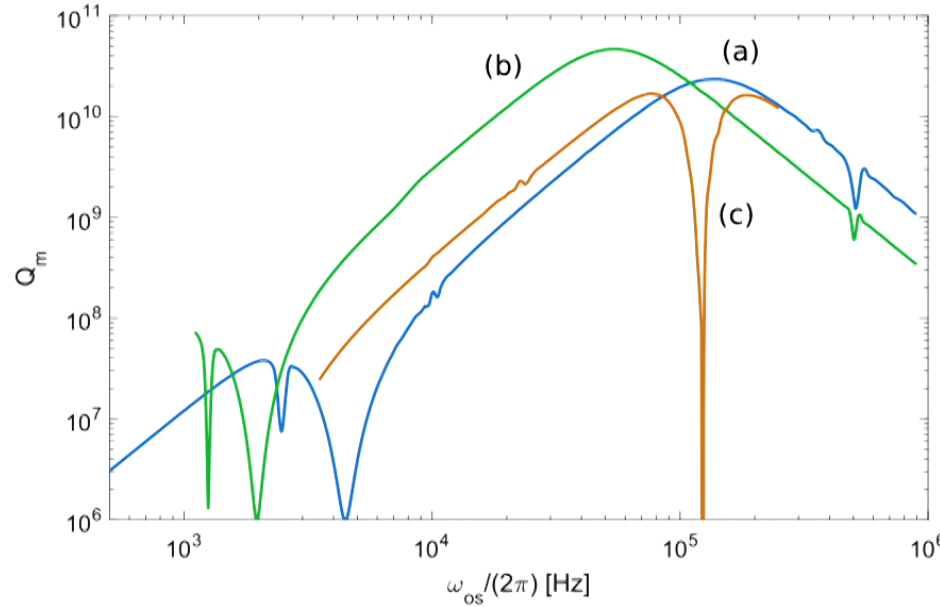
2) Acceleration loss: the optical spring force exciting the internal mode and the energy lost because of mechanical loss of the material.



Path to kHz GW detectors

Mechanical resonators: acc. loss

36

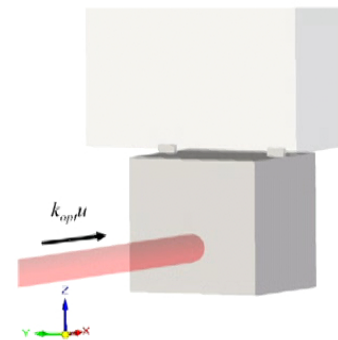


(a): $30 \mu\text{m}$ square by $10 \mu\text{m}$ thick. $15 \mu\text{m} \times 6 \mu\text{m} \times 25 \text{ nm}$ ribbon suspension.

(b): increase to $50 \mu\text{m}$ square, but other parameters same;

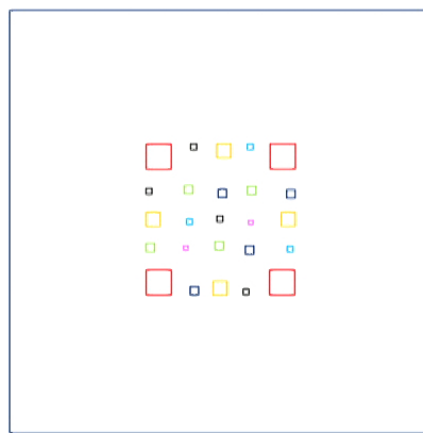
(c): same size mirror as in(a) but the suspension is increased to $30 \mu\text{m}$, which causes a problematic transverse suspension mode near $\omega_{\text{opt}}/(2\pi) = 170 \text{ kHz}$.

Path to kHz GW detectors

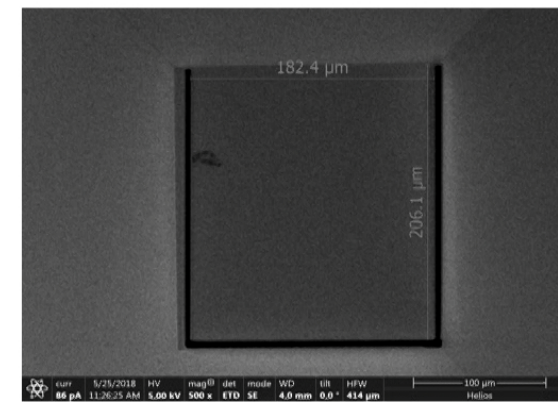


Mechanical resonators: Fabrication

37



- 1160 μm * 1160 μm
- 640 μm * 640 μm
- 400 μm * 400 μm
- 310 μm * 310 μm
- 250 μm * 250 μm
- 185 μm * 185 μm
- 175 μm * 175 μm



Multiple 6 μm thick AlGaAs/GaAs windows on a 0.5mm think silicon frame

The first cantilever using FIB cutting;
The top of the cantilever will be thinned to suspension ribbons.

Path to kHz GW detectors

Mechanical resonators: summary

38

- High Q-factor mechanical resonator to meet the requirements of optomechanical filters is difficult to achieve, but, it is possible in principle
- We are still at the starting point.

Path to kHz GW detectors